Method to classify elderly subjects as fallers and non-fallers based on gait energy image

Ziba Gandomkar, Fariba Bahrami

Motor Control and Computational Neuroscience laboratory, Control and Intelligent Processing Center of Excellence (CIPCE), School of Electrical and Computer Engineering, College of Engineering, University of Tehran, Tehran 14395-515, Iran
E-mail: fbahrami@ut.ac.ir

Published in Healthcare Technology Letters; Received on 6th May 2014; Revised on 19th August 2014; Accepted on 30th August 2014

Falls are one of the leading causes of injuries among the elderly. Therefore, distinguishing fallers and performing preventive actions is vitally important. A new variation of the gait energy image (GEI) called coloured gait energy image (CGEI) is proposed for classifying subjects as fallers and non-fallers and for visualising their gait patterns. Eight elderly fallers, eight elderly non-fallers and eight young subjects performed timed up and go (TUG) test, which is one of the well-known clinical tools for fall risk assessment and contains two gait sequences. Subjects were also asked to perform two other variations of the TUG test, namely TUG with manual load and TUG with cognitive load. Gait sequences were extracted from the TUG test based on the opinion of three human observers. Then the gait cycles were automatically extracted from the walking sequence and divided into three phases, corresponding to double support and first and second half of single support. Next, the GEI of each phase was generated and formed one of the colour components of CGEI. Histogram-based features obtained from CGEI were then used to classify the video collected from walking sequences of elderly fallers and non-fallers. Correct classification rate was improved by approximately 27% compared with the standard TUG test.

1. Introduction: A fall is defined as unintentionally coming to the ground level with a reason other than stroke, epileptic seizure, drug use and sudden unconsciousness [1]. It might cause injuries, fractures, fear of fall and immobility among the elderly people. About one-third of seniors fall each year and more than half of them do not talk about it with their physicians when it occurs [2]. In some studies, automatic sensor-based methods have been proposed to detect falls. For example, in the method presented in [3], a 3D video-based system for monitoring an elderly person to detect fall was proposed. In a more recent study, a two-stage method based on data from the Microsoft Kinect for detecting falls in the homes of the elderly people was presented [4].

However, if the elderly fallers are identified based on their motion patterns and targeted for interventative treatment, the cost associated with fall will decrease extensively. Therefore several tools have been proposed for fall risk assessment and classification of seniors as fallers and non-fallers. Some of the tools assess fall risk based on questionnaires inquiring about fall risk factors and the patient's health status; whereas in the other ones, the subject is asked to perform some pre-defined tasks and the risk of falling is assessed based on the subject's performance in these tests [5]. For scoring how a subject performs the tasks, some of the methods have relied on the clinician's subjective assessment, while the others have suggested more objective criteria by using sensors. In [6], methods based on sensor devices to evaluate functional performance of sit-to-stand and stand-to-sit have been comprehensively reviewed.

Another well-known clinical test for fall risk assessment is timed up and go (TUG) test [7]. In [8], using body-worn kinematic sensors, a quantitative assessment framework for the elderly subject's performance in the TUG test has been proposed. In another attempt, inertial sensors were used to extract features from the TUG test for classification of the elderly as fallers and non-fallers [9]. Body-worn sensors or inertial sensors are relatively expensive. In addition, inertial sensors have to be attached on the subject's body. This may lead to changes in the normal pattern of activities and is annoying, particularly for the elderly. Therefore vision-based markerless systems with inexpensive cameras seem to be desirable. Although in some studies such as [10], different gait parameters have been extracted, there has been limited focus on vision-based methods for identifying differences in gait pattern aiming at classifying the elderly as fallers and non-fallers.

In this Letter, a vision-based markerless gait analysis method for classification of the elderly subjects as fallers and non-fallers is proposed. The presented method is a novel modification of gait energy image (GEI). GEI, first introduced in [11] for gait identification, gives implicit cues about gait patterns. Its main advantages are robustness to error in silhouette extraction and low computational cost. Its main drawbacks are sensitivity to camera angle and lack of temporal information. To overcome the latter, GEI has been modified in this study.

2. Dataset: In this study, an elderly faller was a person older than 65 years who had fallen twice or more in the last year. The characteristics of the subjects are summarised in Table 1. Each subject was asked to perform the TUG test in front of a camera three times. In the TUG test, the subject is asked to rise from an armless chair, walk three meters, turn 180°, walk back to the starting point, and sit down again. Two walking sequences of the TUG test were extracted and used for CGEI computation. In this study, we used the TUG test to compare our proposed method with the TUG test as an example of a commonly used tool for fall risk assessment in terms of their faller/non-faller classification ability. In the conventional TUG test, fall risk is assessed only by measuring the total time of the test. Therefore, we also recorded the total time to perform the TUG test for comparison purposes.

Table 1 Characteristics of subjects

	Young subjects	Non-faller	Faller
no.	8	8	8
age, year	25.4 ± 1.1	68.9 ± 3.2	71.8 ± 3.2
weight, kg	72.1 ± 8.8	61.1 ± 4.5	60.9 ± 2.7
height, cm	175.6 ± 6.1	165.9 ± 3.9	165.0 ± 4.9

doi: 10.1049/htl.2014.0065

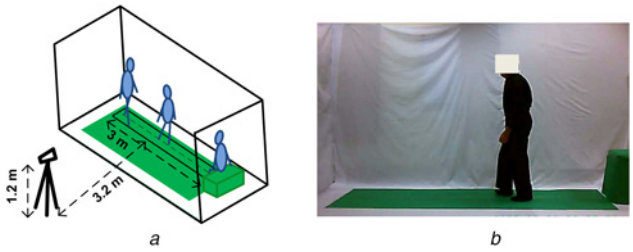

Figure 1 *Installed setup for data collection and frame of recorded video from faller subject*
a Installed setup
b One frame of recorded video

The data were collected at the Motor Control and Computational Neuroscience Laboratory at the University of Tehran. Eight fallers, eight non-fallers, and eight young subjects (control group) participated in this study. Subjects performed the test in front of a white background and were asked to do their best to follow the straight path on the floor, which was made using transparent tape. The floor was green; the distance between the camera and the centre of the path was 3.2 m and the camera height was 1.2 m. Fig. 1*a* shows the installed setup for data collection. The spatial resolution of the camera was 640 × 480 pixels and its frame rate was 25 frames per second. All subjects were asked to initiate their gait with the camera side leg. Fig. 1*b* shows a faller while performing the test. In addition, subjects were asked to perform two other variations of the TUG test to emulate normal life conditions more concretely. The first variation was the TUG test with manual load in which the subjects performed the TUG test while carrying a glass of water and the second variation was the TUG test with cognitive load in which subjects accomplished TUG while doing a mental task, that is, counting backwards from a random number greater than 50 with a specified step size [7].

Finally, 216 video sequences of the TUG tests were collected (24 subjects, each performed three variations of the test three times). In addition, 120 background frames had been collected before each subject performed each test and labelled as background videos. Therefore the database included 216 background videos. Visual inspection was used to validate the method. In order to reduce the error of human observation, we asked three observers to inspect the videos instead of one. First, the observers were asked to find frames corresponding to the start and end of walking in each sequence. Secondly, the observers were asked to mark heel contact and toe clearance.

All observers were M.Sc. students at the University of Tehran. Software was developed in MATLAB and utilised for showing the videos to the observers and recording the results of their visual inspection. They could stop or replay the video as many times as they wanted and were allowed to zoom in on any selected frame to evaluate it more precisely. They were also able to move the video backwards and forwards frame by frame and insert a datatip text box to display the *x*- and *y*-coordinate values of any desired point.

The toe off and heel contact times were clearly defined for the observers at the beginning. As suggested in [12], we defined the heel contact time as the time when the heel stops moving temporarily, and toe off as the time in which the toe position starts to change after being unchanged for a period of time. Using the datatips and zoom option, the observers could inspect the toe and heel positions frame by frame. We asked the observers to consider the foremost point of the foot as toe and the posterior end of the foot as heel. The observers were blind to the labels of 'faller' and 'non-faller' and could spend as much time as they needed to inspect the video. Suggested frames of all observers were averaged for each video sequence and videos of walking were trimmed accordingly. By averaging the reported frames, the overall error was reduced. Since two walking sequences exist in each TUG test, a total of 432 videos were collected.

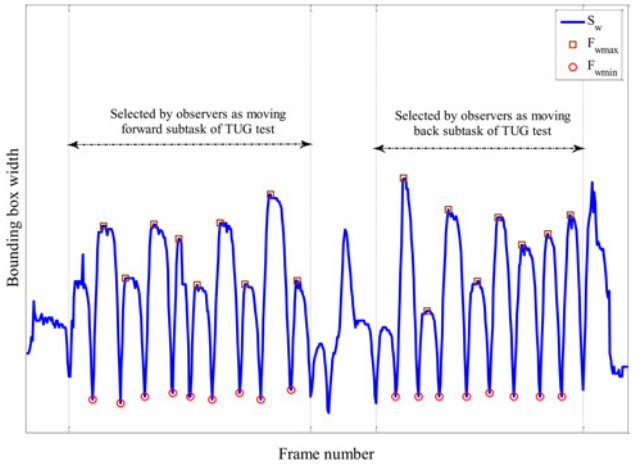

Figure 2 *Width of the one-third lower part of the silhouette (S_w) against frame number in whole frames of a TUG test for a faller subject*

3. Silhouette extraction: In each frame, the background was removed by means of thresholding the Mahalanobis distance of the pixels from the background statistics. Each background pixel was assumed to have a normal distribution. The mean and standard deviation of the background pixels for each test video were calculated using the background videos. After thresholding, some undesired regions remained due to noise and shadows on the floor. The noise was removed by utilising morphological operators and omitting the scattered regions far from the largest connected component (silhouette). To restrict the extracted foreground to the silhouette and eliminate the shadows on the floor, the angle between the *G*-axis and RGB vector for each extracted pixel of the lower part of the silhouette was found. The pixels with angles less than 150 were excluded from the silhouette. The underlying reason for using this procedure for shadow removal was the fact that the proportion of different colour components of a shadow pixel on the floor is nearly identical to the floor pixels. As a result, the angle between the *G*-axis and the RGB vector of a shadow pixel is almost equal to zero although the norm of an RGB vector of a floor pixel and a shadow pixel might differ considerably.

4. Conventional GEI: First the heights of all silhouettes were normalised. To align the silhouettes for each walking sequence, the images were transferred so that the centre of the trunk became the centre of the image. GEI(x, y) was built by averaging all aligned silhouettes using the following equation

$$\mathrm{GEI}(x, y) = \frac{1}{N}\sum_{n=1}^{N} B_n(x, y) \tag{1}$$

where $B_n(x, y)$ is the aligned silhouette in the nth frame and N represents the total number of frames. In $B_n(x, y)$, if a pixel belongs to the silhouette, its value is one, otherwise its value is zero.

5. Coloured gait energy image (CGEI): To fuse temporal information to GEI, each gait cycle was divided into three parts, namely DS, SS1, SS2 and the GEI was computed for each part separately. At first, the bounding box of the one-third lower part of the silhouette in each frame was found and S_w, which was an array containing the bounding box width of all frames, was built. We have not used the width of the whole body, since in many cases the width of the bounding box corresponding to the whole silhouette had remained almost unchanged particularly during the TUG test with manual load since the subject was carrying a glass. S_w is plotted in Fig. 2 against the frame number. Local

minima and maxima of S_w that are more than 20 frames apart are marked.

The flowcharts depicted in Figs. 3*a* and *b* show the procedure for extracting F_{HC} and F_{TO}, respectively, which were later used for CGEI generation. In these flowcharts, $F_{W\mathrm{min}}$ and $F_{W\mathrm{max}}$ correspond to the local minima and maxima of S_w and (*condition*)? test, whether the *condition* has been fulfilled or not. Just the one-seventh lower part of the silhouette was considered to evaluate if a swing foot passed the stance foot, as according to anthropometric data, half of the knee-heel length is nearly one-seventh of the body height. Fig. 3*c* shows the location of pixels of interest for lowermost and headmost as described in flowcharts. A few frames after and before F_{HC}, in which the lowermost pixel of the front foot (an approximation for heel) stopped moving temporarily, are shown in Fig. 4*a*. Similarly, a few neighbouring frames of F_{TO} are depicted in Fig. 4*b*. In Fig. 5*a*, *x*–*y* coordinates of the lowermost pixel of the front foot is plotted against the frame number. F_{HC} is marked in this figure. Moreover, as depicted in Fig. 5*b*, the frame in which the position of the headmost pixel of the back foot (an approximation for toe) changed dramatically after being stationary for a while was labelled as F_{TO}.

F_{TO} and F_{HC} are almost equal to the heel contact and toe off times, respectively. These events are important in gait analysis as they are used to divide gait into two phases. Double support phase starts from heel contact of the front foot and ends with toe off of the back foot while single support starts from toe off until heel contact of the same foot. Having the definition of the gait phases in mind, we divided each step into three parts: DS (almost equal to double support phase), SS1 (almost equal to the first half of the single support), and SS2 (almost equal to the second half of the single support). In the next step, GEI is computed for each part of each step using (2)–(4).

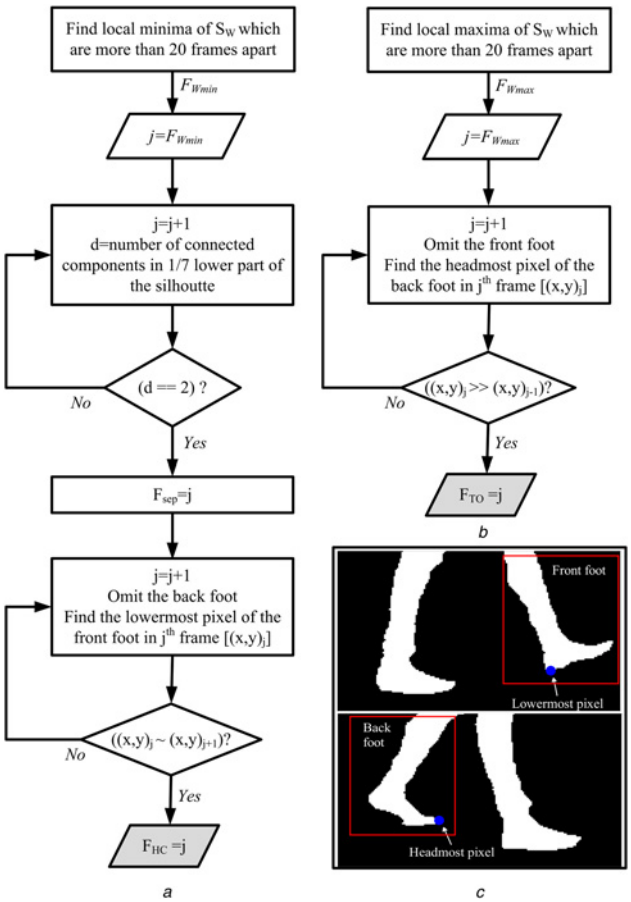

Figure 3 *Procedure of finding F_{HC} and F_{TO} and pixels of interest of two sample forms*
a F_{HC}
b F_{TO}
c Headmost and lowermost pixels of two sample frames

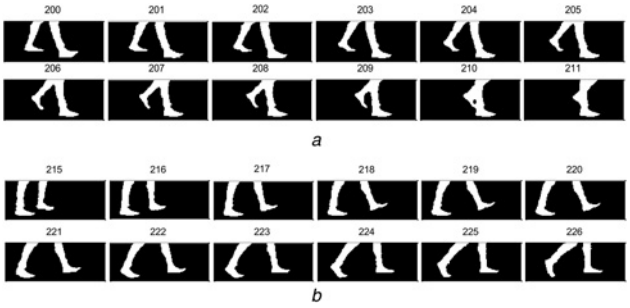

Figure 4 *Neighbouring frames of F_{HC} and F_{TO}*
a F_{HC}
b F_{TO}
The frame number is stated above each image

$$\mathrm{CGEI}_{\mathrm{DS}}(x,y) = \sum_{F_{\mathrm{HC}_1}}^{F_{\mathrm{TO}}} B_n(x,y) \tag{2}$$

$$\mathrm{CGEI}_{\mathrm{SS1}}(x,y) = \sum_{F_{\mathrm{TO}}+1}^{F_{w\min}} B_n(x,y) \tag{3}$$

$$\mathrm{CGEI}_{\mathrm{SS2}}(x,y) = \sum_{F_{w\min}+1}^{F_{\mathrm{HC2}-1}} B_n(x,y) \tag{4}$$

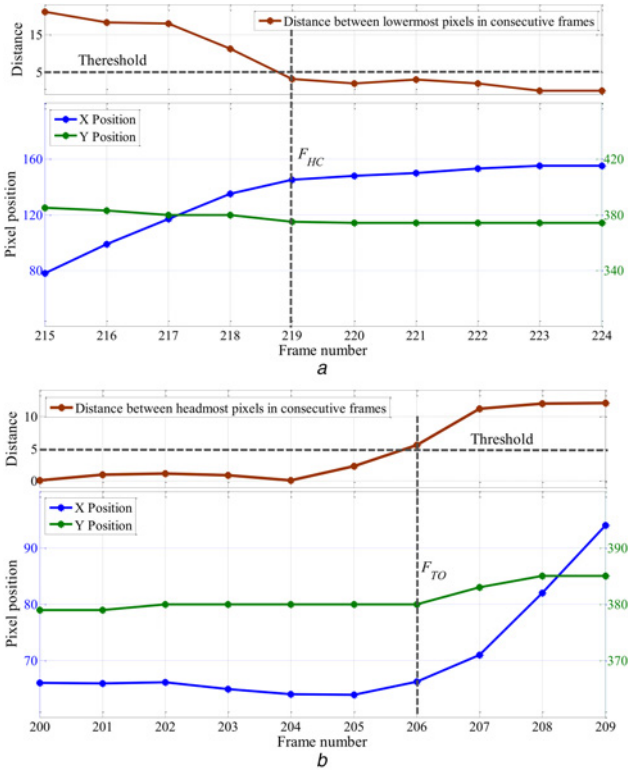

Figure 5 *Example of X–Y position pixel against frame number*
a Lowermost pixel of front foot
b Headmost pixel of back foot

doi: 10.1049/htl.2014.0065

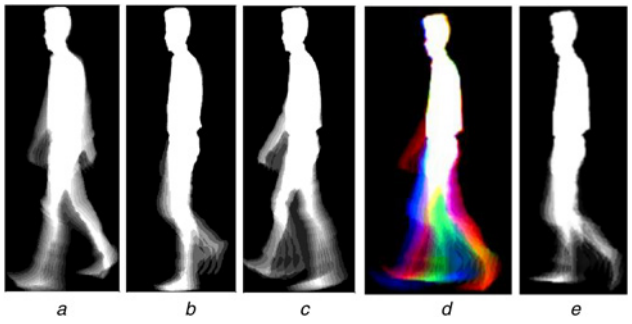

Figure 6 *$CGEI_{DS}$, $CGEI_{SS1}$ and $CGEI_{SS2}$ (a–c) CGEI and GEI (d, e)*
a $CGEI_{DS}$
b $CGEI_{SS1}$
c $CGEI_{SS2}$
d CGEI
e GEI

$CGEI_{DS(x,\ y)}$, $CGEI_{SS1(x,\ y)}$ and $CGEI_{SS2(x,\ y)}$ are the GEI for DS, SS1 and SS2. F_{HC1} and F_{HC2} represent frames corresponding to two consecutive steps (one stride). $CGEI_{DS}$, $CGEI_{SS1}$ and $CGEI_{SS2}$ for a single step are shown in Figs. 6*a–c*, respectively. To visualise the new variation of GEI, $CGEI_{DS}$, $CGEI_{SS1}$ and $CGEI_{SS2}$ were considered as red, green and blue components, respectively of a new image called CGEI. The CGEI is compared with GEI in Figs. 6*d* and *e*. The final CGEI was built by averaging the obtained CGEI for all steps.

As the final aim of this Letter was to discriminate between the gait of elderly fallers, who sometimes suffers from asymmetric gait, two CGEIs were built for each walking sequence. In the first one, $(CGEI)_{Left}$, we averaged CGEIs of all steps starting from the left foot heel contact, while in the second one, $(CGEI)_{Right}$, we averaged CGEIs of all steps starting from the right foot heel contact. To cancel the impact of subjects' clothes and body size, the value of all stationary parts of CGEI (white areas) was set to zero, forming masked CGEI. CGEIs and masked CGEIs of an elderly faller and non-faller are depicted in Fig. 7.

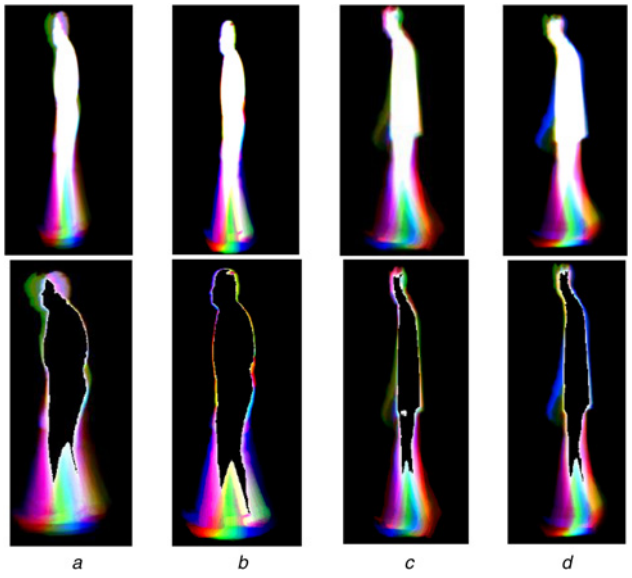

Figure 7 *$(CGEI)_{Left}$ and $(CGEI)_{Right}$ of faller and non-faller subjects*
a $(CGEI)_{Left}$ of faller subject
b $(CGEI)_{Right}$ of faller subject
c $(CGEI)_{Left}$ of non-faller subject
d $(CGEI)_{Right}$ of non- faller subject
In all cases, CGEI and masked CGEI are shown in top and bottom, respectively.

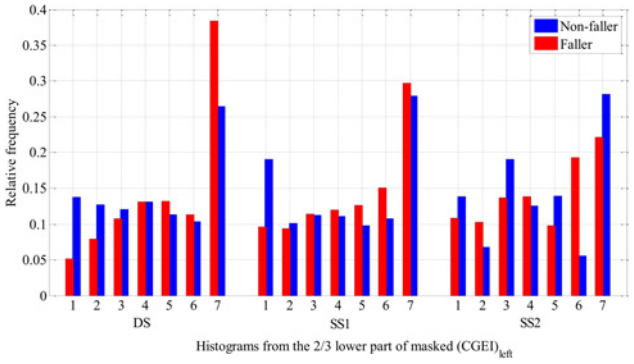

Figure 8 *Extracted features for a faller and a non-faller by concatenating the histograms of three components of $(CGEI)_{Left}$*

6. Feature extraction and classification: In GEI, the higher grey level shows that the pixel remains stationary for a longer time. Therefore the number of pixels in each bin of the grey-level histogram implicitly gives cues about the subject's gait pattern. As the head and the upper part of the trunk are almost still in comparison to the feet, we generated the eight-bin grey level histograms just for the two-third lower part of the silhouette. The histograms of all components of $(CGEI)_{Left}$ and $(CGEI)_{Right}$ were found separately for each gait sequence. The first bin, which was corresponding to the 'zero' grey-level value, was omitted as it was associated with background pixels.

After omitting the first bin, all histograms were normalised so that the area under the histogram became one. For each gait sequence, three feature vectors were built. To generate the first one, the normalised grey-level histogram of the two-third lower part of conventional GEI was built. The histogram of the two-third lower part of each component of $(CGEI)_{Left}$ and $(CGEI)_{Right}$ was generated separately and then concatenated to build the second feature vector. The third feature vector was built similar to the second one by using masked $(CGEI)_{Left}$ and $(CGEI)_{Right}$. Extracted features for a faller and a non-faller from $(CGEI)_{Left}$ is shown in Fig. 8.

The dimension of all feature vectors was reduced to three using principle component analysis (PCA). Support vector machine

Table 2 Error (%) for faller/non-faller, faller/young and young/non-faller detection

Classification to:	Faller/ non-faller	Faller/ youth	Youth/ non-faller
Mean of entire test duration (threshold with the lowest error is considered)			
standard	37.5	25	50
manual load	31.2	25	43.7
cognitive load	25	18.75	43.7
Proposed feature from GEI			
standard	35.4	20.8	39.6
manual load	31.2	22.9	41.6
cognitive load	29.1	18.75	39.6
Proposed feature vector 2			
standard	16.7	12.5	20.1
manual load	6.2	8.3	25.0
cognitive load	6.2	10.4	20.1
Proposed feature vector 3			
standard	10.4	8.3	18.7
manual load	6.2	6.2	22.9
cognitive load	4.2	4.2	14.6

Table 3 Percentage error, sensitivity, specificity, PPV and NPV of detecting a faller using histogram-based feature vector obtained from DS1, SS1 and SS2 for the TUG test with cognitive load

	Sensitivity, %	Specificity, %	PPV, %	NPV, %	Error, %
DS	83	83	83	83	16.7
SS1	88	96	95	88	8.3
SS2	75	88	86	78	18.7

(SVM) and leave-one-gait sequence-out cross-validation were utilised to evaluate the performance of the proposed method. Each time, one walking sequence was considered as the test data and all other sequences except those belonging to the same subjects were used as a training dataset. By eliminating all sequences of the subject from the training set, we ensured that the biometric properties of the gait did not boost the classification result.

7. Experimental result: To evaluate the performance of the proposed method in faller/non-faller classification, it was applied on the dataset. As suggested in Section 6 three feature vectors based on GEI, CGEI and masked CGEI were generated for each walking sequence. The error (%) for classification of the elderly subjects as fallers or non-fallers is shown in the first column of Table 2. To evaluate the discriminative ability of the proposed features and its robustness, two other classification tasks were accomplished. In the first one, using the proposed features the elderly fallers were distinguished from the young subjects. In the second task, the proposed method was applied on the data of elderly non-fallers and young subjects and its error is reported in the last column.

As expected, the classification error of the third feature vector was the lowest and over all, the classification error of faller/young subjects was less than other classification tasks. To compare the proposed method with an example of a clinical method which is currently in use for the elderly fall risk assessment, the error for each classification task using the time required to perform the TUG test is also reported in Table 2. The TUG test is currently utilised as a clinical tool for elderly faller detection and normally if the entire time to perform the TUG test is below a threshold, the subject is considered as non-faller. Here for each variation of the test and each classification task, we applied different threshold values to find the one with the lowest error. As shown, the proposed method outperformed the TUG test.

As stated in 2.4 the starting and ending frames for generating $CGEI_{DS(x,y)}$ is almost equal to heel contact and toe off times, which were marked for each step in our dataset by visual inspection. To evaluate the performance of the proposed algorithm in extracting these events, F_{HC} and F_{TO} were compared to the average of the reported frames by three observers for heel contact and toe off. The total number of steps in 432 walking sequences was 3312. The mean-squared error for toe off and heel contact detection was 2.8 and 1.5 frame^2, respectively.

To find the gait phase in which the differences between fallers and non-fallers are more obvious from the silhouette shape, classification was performed using histogram-based features obtained from each phase separately. Since the best result in the previous part was obtained from the TUG test with cognitive load, the classification task was performed just for this test. Sensitivity, specificity, positive predictive value (PPV), negative predictive value (NPV) and error of classification are reported in Table 3.

8. Conclusion: In this Letter, a new modification of GEI, which is called CGEI, has been proposed and used to classify the elderly subjects as fallers and non-fallers and to visualise the walking sequences. It has been demonstrated that the discriminative ability of features extracted from the TUG test with cognitive load is higher than that of the TUG test with manual load and the standard TUG test. In addition, the result suggested that the most impaired gait phase among fallers is SS1. This phase is almost corresponding to toe clearance.

As future work, we are going to use CGEI for abnormal gait detection and gait identification. It should be noted that the proposed method for toe off and heel contact detection was validated by visual inspection of an observer looking at the recorded video images frame by frame, since gait event detection was not the focus of this study. In future, the ability of the method for automatic gait event detection could also be validated using the well-known gait event detection techniques based on foot switches or gait-mats. The main drawback of the proposed algorithm is its sensitivity to the view angle of the camera. In addition, the proposed algorithm uses a simple background model for silhouette extraction. Therefore the method is sensitive to the background and environment light.

9 References

[1] Lord S., Sherringtone C., Menz H.B.: 'Falls in older people: risk factor and strategies for prevention' (Cambridge University Press, Cambridge, UK, 2001)

[2] Stevens J.A., Ballesteros M.F., Mack K.A., Rudd R.A., DeCaro E., Adler G.: 'Gender differences in seeking care for falls in the aged Medicare Population', *Am. J. Prev. Med.*, 2012, **43**, pp. 59–62

[3] Yu M., Yu Y., Rhuma A., Naqvi S.M., Wang L., Chambers J.A.: 'An online one class support vector machine based person-specific fall detection system for monitoring an elderly individual in a room environment', *IEEE J. Biomed. Health Inf.*, 2013, **17**, (6), pp. 1002–1014

[4] Stone E., Skubic M.: 'Fall detection in homes of older adults using the Microsoft Kinect', *IEEE J. Biomed. Health Inf.*, 2014, (99), doi: 10.1109/JBHI.2014.2312180

[5] Gates S., Smith L.A., Fisher J.D., Lamb S.E.: 'Systematic review of accuracy of screening instruments for predicting fall risk among independently living older adults', *J. Rehabil.*, 2008, **45**, (8), pp. 1105–1116

[6] Millor N., Lecumberri P., Gomez M., Martinez-Ramirez A., Izquierdo M.: 'Kinematic parameters to evaluate functional performance of sit-to-stand and stand-to-sit transitions using motion sensor devices: a systematic review', *IEEE Trans. Neural Syst. Rehabil. Eng.*, 2014, (22), doi: 10.1109/TNSRE.2014.2331895

[7] Shumway-Cook A., Brauer S., Woollacott M.: 'Predicting the probability for falls in community-dwelling older adults using the Timed Up & Go Test', *Phys. Ther.*, 2000, **80**, (9), pp. 896–903

[8] Greene B.R., Donovan A.O., Romero-Ortuno R., Cogan L., Scanaill C.N., Kenny R.A.: 'Quantitative falls risk assessment using the timed up and go test', *IEEE Trans. Biomed. Eng.*, 2010, **57**, (12), pp. 2918–2926

[9] Salarian A., Horak F.B., Zampieri C., Carlson-Kuhta P., Nutt J.G., Aminian K.: 'iTUG, a sensitive and reliable measure of mobility', *IEEE Trans. Neural Syst. Rehabil. Eng.*, 2010, **18**, (3), pp. 303–310

[10] Wang F., Stone E., Skubic M., Keller J.M., Abbott C., Rantz M.: 'Towards a passive low-cost in-home gait assessment system for older adults', *IEEE J. Biomed. Health Inf.*, 2013, **17**, (2), pp. 346–355

[11] Han J., Bhanu B.: 'Individual recognition using gait energy image', *IEEE Trans. Pattern Anal. Mach. Intell.*, 2006, **28**, (2), pp. 316–322

[12] Ghoussayni S., Stevens C., Durham S., Ewins D.: 'Assessment and validation of a simple automated method for the detection of gait events and intervals', *Gait Posture*, 2004, **20**, (3), pp. 266–272

doi: 10.1049/htl.2014.0065